

# GIS-based landslide susceptibility mapping with logistic regression, analytical hierarchy process, and combined fuzzy and support vector machine methods: a case study from Wolong Giant Panda Natural Reserve, China

Qingkai Meng<sup>1</sup>  · Fang Miao<sup>1</sup> · Jing Zhen<sup>2</sup> · Xinyuan Wang<sup>2</sup> · An Wang<sup>3</sup> · Ying Peng<sup>4</sup> · Qiang Fan<sup>5</sup>

Received: 27 March 2015 / Accepted: 17 August 2015 / Published online: 2 September 2015  
© Springer-Verlag Berlin Heidelberg 2015

**Abstract** Landslides, as one of the most destructive natural phenomena, distribute extensively in Wolong Giant Panda Natural Reserve and cause damage to both humans and endangered species. Therefore, landslide susceptibility zonation (LSZ) mapping is necessary for government agencies and decision makers to select suitable locations for giant pandas. The main purpose of this study is to produce landslide susceptibility maps using logistic regression (LR), analytical hierarchy process (AHP), and a combined fuzzy and support vector machine (F-SVM) hybrid method based on geographic information systems (GIS). A total of 1773 landslide scarps larger than one cell ( $25 \times 25 \text{ m}^2$ ) were selected in the landslide inventory mapping, 70 % of which were selected at random to be used as test data, and the other 30 % were used as validation. Topographical, geological, and hydrographical data were collected, processed, and constructed into a spatial database. Nine conditioning factors were chosen as influencing factors related to landslide occurrence: slope

degree, aspect, altitude, profile curvature, geology and lithology, distance from faults, distance from rivers, distance from roads, and normalized difference vegetation index (NDVI). Landslide susceptible areas were analyzed and mapped using the landslide occurrence factors by different methods. For conventional assessment, weights and rates of the affecting factors were assigned based on experience and knowledge of experts. In order to reduce the subjectivity, a combined fuzzy and SVM hybrid model was generated for LSZ in this paper. In this approach, the rates of each thematic layer were generated by the fuzzy similarity method, and weights were created by the SVM method. To confirm the practicality of the susceptibility map produced by this improved method, a comparison study with LR, AHP was assessed by means of their validation. The outcome indicated that the combined fuzzy and SVM method (accuracy is 85.73 %) is better than AHP (accuracy is 78.84 %), whereas it is relatively similar to LR (accuracy is 84.55 %). The susceptibility map based on

---

✉ Qingkai Meng  
mengqk@cdut.edu.cn

Fang Miao  
mf@cdut.edu.cn

Jing Zhen  
zhenjing@radi.ac.cn

Xinyuan Wang  
wangxy@radi.ac.cn

An Wang  
amturing@outlook.com

Ying Peng  
ypeng@cdut.edu.cn

Qiang Fan  
fanq@cdut.edu.cn

<sup>1</sup> College of Geophysics, State Key Laboratory of Geohazard Prevention and Geoenvironment Protection, Key Lab of Earth Exploration & Information Techniques of Ministry of Education, Chengdu University of Technology, Chengdu 610059, China

<sup>2</sup> Center for Earth Observation and Digital Earth, Chinese Academy of Sciences, Beijing 100094, China

<sup>3</sup> College of Information Science and Technology, Chengdu University of Technology, Chengdu 610059, China

<sup>4</sup> College of Nuclear Technology and Automation Engineering, Chengdu University of Technology, Chengdu 610059, China

<sup>5</sup> State Key Laboratory of Geohazard Prevention and Geoenvironment Protection, Chengdu University of Technology, Chengdu 610059, China

combined the fuzzy and SVM approach also shows that 5.8 % of the study area is assigned as very highly susceptible areas, and 17.8 % of the study area is assigned as highly susceptible areas.

**Keywords** Landslide susceptibility map · Wolong Giant Panda Natural Reserve · GIS · Combined fuzzy and SVM

## Introduction

Wolong Natural Reserve is one of the largest habitats for giant pandas in the world. This region was listed as one of the world's top 25 biodiversity hotspots by Conservation International, and named as a Global 200 eco-region by the World Wildlife Fund, and inscribed as a World Heritage Site in 2006 (UNESCO World Heritage Center 2006). Wenchuan earthquake (May 12, 2008) triggered abundant secondary landslides and created unstable landslide areas, which have threatened the ecological environment for giant pandas in Wolong Natural Reserve (Ouyang et al. 2008). Therefore, landslide susceptibility zonation (LSZ) of this area is an urgent subject for future decision makers to select the low susceptible areas of landslide hazards as suitable locations for giant pandas.

In order to assess landslide hazards and construct maps portraying their spatial distribution, many researchers have attempted to use different methods, either qualitative or quantitative (Aleotti and Chowdhury 1999; Guzzetti et al. 1999; Dai and Lee 2002; Ayalew and Yamagishi 2005). Qualitative methods represent the susceptible level based on expert opinion. Scholars used these methods very frequently in the 1970s (Carrara and Merenda 1976; Fenti et al. 1979; Kienholz 1978; Ives and Messerli 1981; Rupke et al. 1988). To minimize the subjective bias from the experts, quantitative methods, such as bivariate statistical, multivariate statistical, and probabilistic prediction models were developed (Corominas et al. 2014). In the meantime, geographical information systems (GIS), with the availability of integrating various thematic layers, became increasingly popular. Many researchers have done landslide susceptibility mapping by rating, weighting, and superimposing various thematic maps corresponding to the causative factors based on GIS, such as probabilistic models (Rowbotham and Dudycha 1998; Luzi et al. 2000; Lee and Min 2004; Akgun et al. 2008, 2011; Ozdemir 2009; Yilmaz 2010a; Oh and Lee 2010, 2011; Pourghasemi et al. 2012a, b; Mohammady et al. 2012), bivariate statistics (Brabb et al. 1972; Yilmaz and Yildirim 2006; Constantin et al. 2011; Yilmaz et al. 2012; Yalcin et al. 2008, 2011; Magliulo et al. 2008; Lucà et al. 2011), multivariate analysis (Carrara 1983; Chung et al. 1995; Santacana et al. 2003; Komac 2006; Piegari et al. 2009; Pradhan et al.

2010a; Nandi and Shakoor 2010), logical regression (Dai et al. 2001, 2003, 2004; Lee and Min 2001; Lee and Pradhan 2007; Can et al. 2005; Yesilnacar and Topal 2005; Goesevski et al. 2006; Lee and Evangelista 2006; Nefeslioglu et al. 2008a; Yilmaz 2009; Lei et al. 2011; Pradhan et al. 2008, 2010a, b, 2011a, b; Chauhan et al. 2010; Bai et al. 2010; Akgun et al. 2012; Bui et al. 2011a; Felicisimo et al. 2013; Süzen and Kaya 2012), and the analytical-hierarchy process (Ayalew et al. 2004; Yoshimatsu and Abe 2006; Ercanoglu et al. 2008; Akgun and Türk 2010; Pourghasemi et al. 2012c; Kayastha et al. 2013).

In recent years, machine learning approaches such as artificial neural networks (ANN) and support vector machines (SVM) have been partially successfully implemented with the advantage of overcoming the deficiency of statistical methods that require two class samples (Pradhan B et al. Pradhan 2010c, d; Sezer et al. 2011; Oh and Pradhan 2011; Tien et al. 2012; Micheletti et al. 2013; Yao et al. 2008; Yilmaz 2008, 2010a; Yilmaz and Yuksek 2008a, b; Polykretis et al. 2015).

Proposed as indirect assessment strategies that combine the advantages of quantitative and qualitative assessments, hybrid models have become the new research hot issue recently, with the intent to create an improved and objective model. Kanungo et al. (2006), Lee et al. (2009) and Vahidnia et al. (2010) have combined a fuzzy inference system (FIS) with an artificial neural network (ANN) to generate LSZ. Goesevski et al. (2006) have integrated fuzzy logic with AHP. Tehrany et al. (2013) applied an ensemble rule based on decision tree (DT) and multivariate statistical methods in the spatial prediction of flood areas in Malaysia. Damasevicius et al. (2010) pointed out that robustness and clustering algorithms can be positively affected by combining grammar inference and SVM.

The hybrid methods cited above give rise to new thoughts of combining two different models together in order to reduce the sensitivity to noises and isolated samples, thus appealing for many scholars (Pradhan 2010a). The combined fuzzy similarity and SVM (F-SVM) method is an improved algorithm for SVM, which can overcome the weakness of either approach. However, attempts to create F-SVM are relative few.

In this paper, the F-SVM method has been created here for landslide susceptibility mapping in Wolong Giant Panda Natural Reserve. Nine factors were selected as landslide controls factors: slope, aspect, altitude, geology, and lithology, distance from rivers, distance from roads, distance from faults, profile curvatures, normalized difference vegetation index. They were constructed based on ArcGIS software for data spatial analysis and manipulation. Then, LSZ was generated and compared with three different approaches (LR, AHP, F-SVM). Finally, the result based on the optimum method in this particular study area could provide

practical suggestions for government and decision makers for future conservation of the giant panda.

## The study area

### General characteristics

Wolong Natural Reserve is a suitable living environment for endangered species, especially for giant pandas. It is located in the west of Sichuan province, China, approximately between  $102^{\circ}52'00''\text{E}$  and  $103^{\circ}25'00''\text{E}$  longitude, and  $30^{\circ}45'00''\text{N}$  and  $31^{\circ}25'00''\text{N}$  latitude, with an area of approximately  $3600\text{ km}^2$ . The epicenter of the Wenchuan earthquake is located 30 km northeast of the study area, dissecting the rock masses into small blocks. The fault zones near well-known Longmenshan mountain fault zones include, from northwest to southeast, Pitiao river fault, Gengda fault, and Yingxiu fault characterized by a series of parallel folds and faults that extend NE  $40\text{--}50^{\circ}$ . The rocks in this area are intensively fractured, and a number of joint sets are developed. The elevation ranges from 1194 to 5789 m. Slope degree in this region is very steep, varying from  $0^{\circ}$  to  $86.117^{\circ}$ . Owing to the particular geographical position and complex geological structure, it is frequently subjected to landslides (Fig. 1).

### Geological setting

The rocks outcropping in the study area range in age from the Early Paleozoic era to Mesozoic. The formation of Jurassic and Cretaceous in Mesozoic is missing, and tertiary units in Cenozoic are also sparse. The Maoxian Group of Silurian is formed of celadon sericite phyllite, silver sand phyllite with a thin layer of quartzite, and thin-bedded and lenticular crystalline limestone in the southeast of the study area along Pitiao River. Triassic formations are distributed in the northwest along the Pitiao River, consisting of feldspar quartz sandstone, slate, carbonaceous phyllite, thin-bedded limestone, and fine siltstone. Additionally, the Jinning-Chengjing formation in the Proterozoic period is distributed in the northeast of the study area and is mainly composed of diorite and granodiorite, with the characteristic of being densely jointed and crushed. Since it is the oldest formation and susceptible to weathering, large numbers of landslides are observed in these units through field investigation.

### Hydrological characteristics

The climate of the study area is very humid. According to the data obtained from a local meteorological station, the average humidity is up to 80 %. The average annual pre-

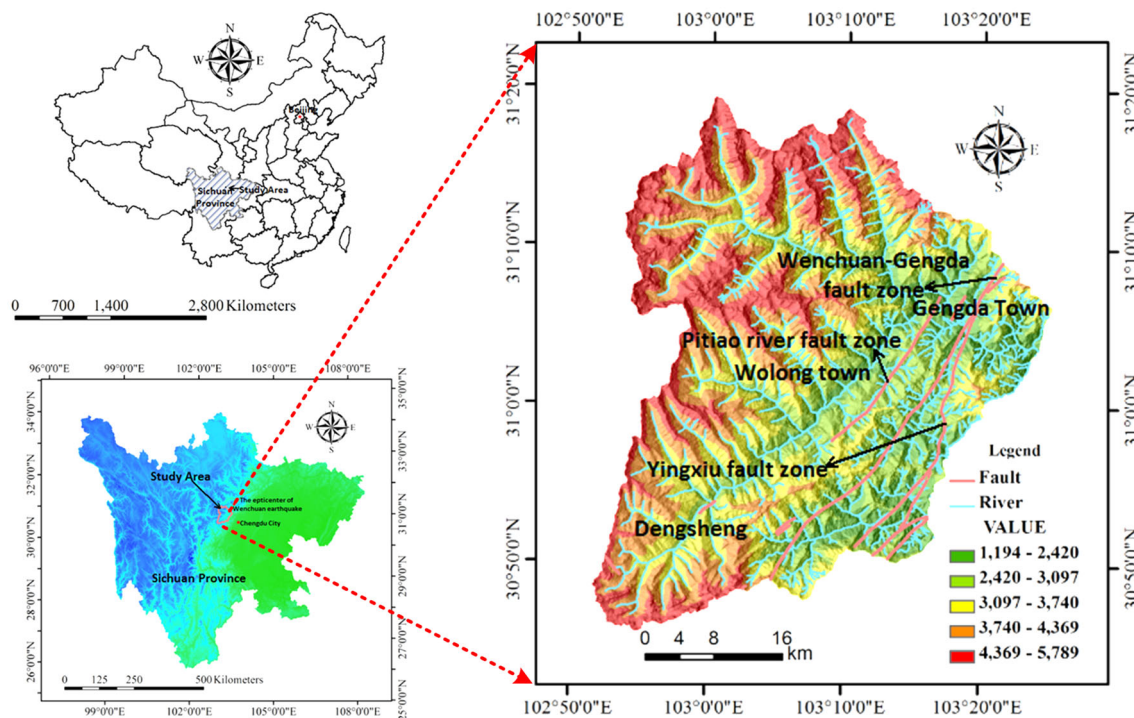


**Fig. 1** Study area

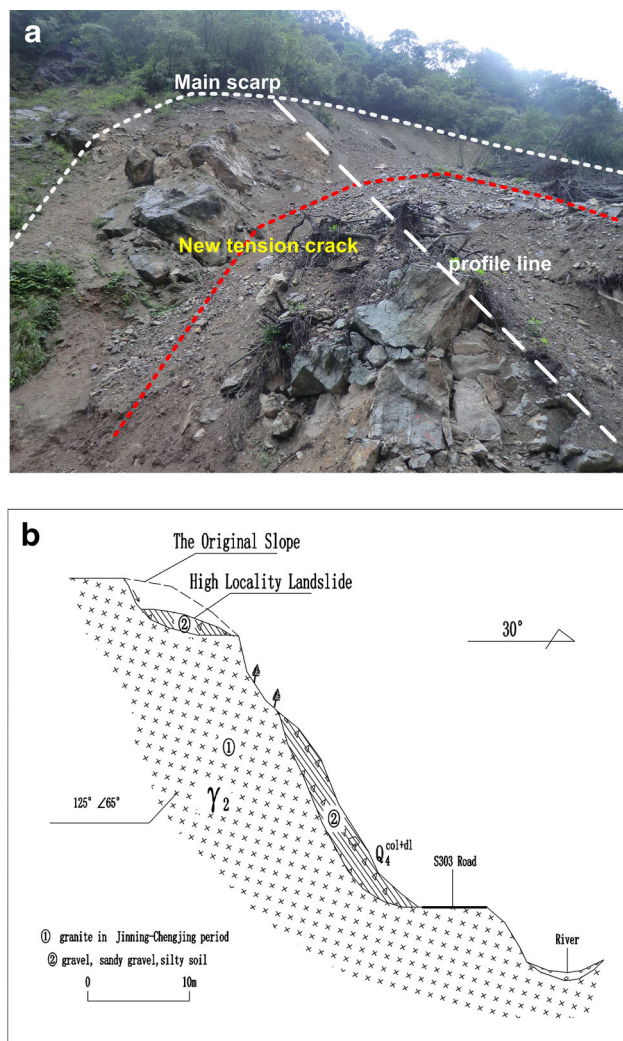


**Fig. 2** a A typical landslide in the study area. b A profile map of a typical landslide in the study area

precipitation is 890 mm and generally concentrates in spring and summer. The main streams in the study area are Pitiao, Jin, Zhong, and Xi rivers. These rivers and their tributaries form a dendritic drainage pattern due to topographical and geological features of the study area.

### Slope failures

Landslides that have occurred in this region are widely distributed and represent a serious threat to humans and giant pandas. Large scales of potential landslides and detrital materials formed on the slope during the process of the earthquake. The rock mass on the slope has become loose after the earthquake and, therefore, provides source material for a potential precipitation-induced landslide. These unstable slopes are very likely to slide when triggered by rainstorms or earthquakes. The following Fig. 2

shows that a landslide with an approximate 70 m length, 50 m width, and 40 m height occurred just after a heavy rainfall. The main body is presumed to be created by the May 12, 2008 Wenchuan earthquake. After heavy rain on June 19, 2014, new tension cracks appeared at the back of the main scarp. As material accumulated, movement accelerated and secondary landslide occurred. Many similar landslides are cited for the study area.

### Construction of a landslide spatial database

For the landslide susceptibility mapping, the primary step is to construct the spatial database from relevant landslide conditioning factors. This stage is thought to be the most important part of landslide susceptibility and hazard mitigation studies (Guzzetti et al. 1999; Ercanoglu and Gokceoglu 2004; Kincal et al. 2009). The spatial database for the study area is composed of slope degree, aspect, altitude, profile curvature, geology and lithology, distance from faults, distance from rivers, distance from roads, and the normalized difference vegetation index (NDVI). These spatial conditioning factors make the slope susceptible without trigger conditions and thus are considered responsible for the occurrence of landslides in the study area. As we know, rainfall and earthquakes, as triggering factors and temporal phenomena, set off the movement by shifting the slope from the quasi-stable state to an unstable state. However, past data on these trigger factors in relation to landslide occurrence are not available and thus are not considered in this study. The sources of this spatial database are shown in Table 1.

In this paper, a digital elevation model (DEM) with a ground resolution of 25 m was constructed by interpolation of 1:50,000 scale local digital contour lines using ArcGIS software. Some significant terrain attributes such as slope gradient, aspect, altitude, and profile curvature were derived from this DEM. All other digital lines such as geology maps, fault distribution, river distribution, and road distribution were converted into raster format and resampled with the same pixel size as the DEM.

### Landslide inventory map

Since a reliable landslide inventory map plays the most important role in mapping the landslide susceptibility, it is necessary to determine the locations and outlines of landslides accurately (Pradhan and Lee 2007). However, employing field survey and observation as the initial method is difficult and time consuming on account of complex and dangerous terrain conditions after the earthquake. Instead, remote sensing methods, such as high resolution remote sensing and aerial photographs, are used to

**Table 1** The source of spatial database used in landslide susceptibility analysis

Classification	Sub-classification	Source	Scale
Geological map	Geology lithology, fault	Geology Survey of Sichuan province	1:200,000
Topographic map	DEM, road	National Cartographic Center	1:50,000
Hydrographical map	River	National Cartographic Center	1:50,000

exact significant and cost effective information on landslides. Certainly, a field survey can be used to verify the result of aerial photograph interpretation and remote sensing imagery analysis.

It should be noted that different sample strategies representing the landslide have different results and have different meanings as well (Nefeslioglu et al. 2008b). Nevertheless, the conceptual differentiation of sampling strategies applied in susceptibility evaluation is commonly ignored. Moreover, there is no agreement on the technique of producing a landslide inventory map. Generally, point, seed cell (Süzen and Doyuran 2004; Yesilnacar and Topal 2005; Sujatha et al. 2012), and scarp (Clerici et al. 2006) are used as training data to represent the failure condition of landslides by researchers. Yilmaz (2010b) has first compared the effect of these three different sampling strategies by means of landslide inventory on a landslide susceptibility assessment, and the result showed

that the scarp sampling strategy performed better than the other two sampling strategies. According to Yilmaz (2010b), the point sampling strategy described by a single X, Y coordinate couldn't reflect the landslide affected area. As is well known, two genetically and morphologically distinct zones can be identified: the depletion zone (the upper part of the landslide where the failure is effectively generated) and the accumulation zone (the lower part which is simply affected by the arrival of the depleted material) (Clerici et al. 2006). If the whole landslide is considered in assessing landslide susceptibility, the accumulation zones are erroneously considered to be prone to landsliding. The depletion zone is generally difficult to identify completely since it is partially occupied by the displaced material. Thus, the main scarp (the higher portion of depletion zone, especially its upper edge) is the most evident morphological feature of a landslide and can be easily distinguished from the

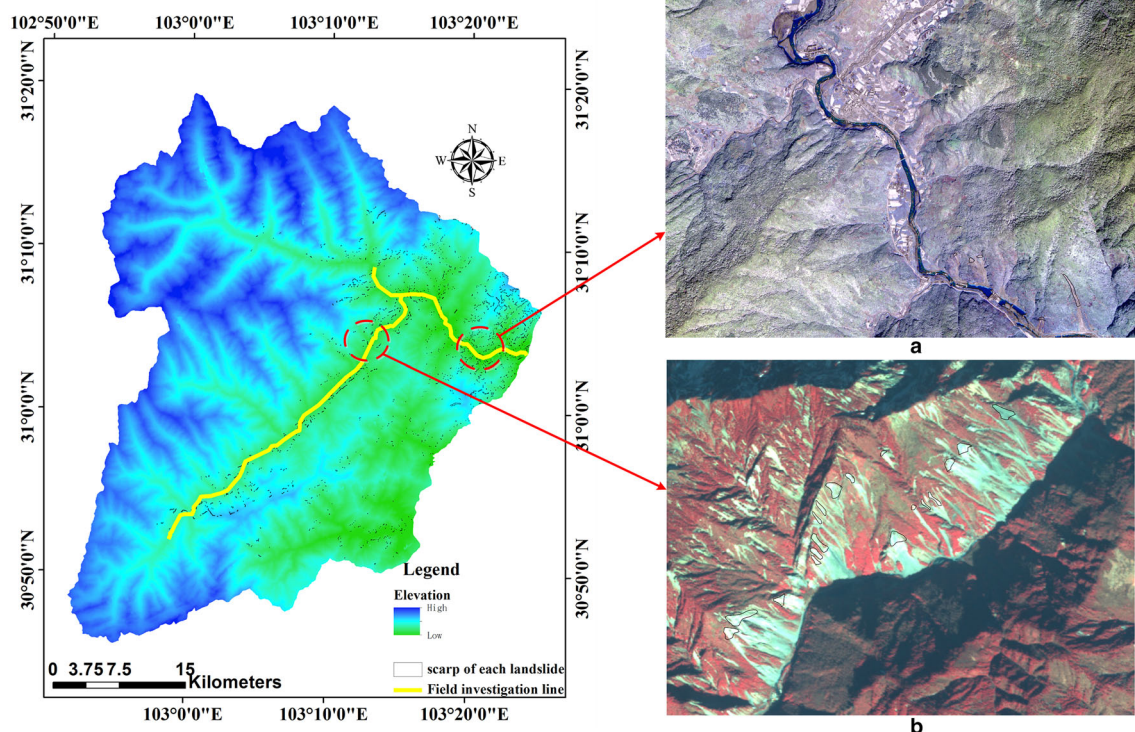


**Fig. 3** Landslide inventory map. **a** The main scarp of landslides were analyzed from IKONOS; **b** the main scarp of landslides were interpreted from SPOT

accumulation/depletion zone or rupture zone as a polygon feature (Yilmaz 2010b) (Fig. 3).

Different map scales (large, medium, and small scales) should be considered in general natural hazard zonation (Holec et al. 2013). Concerning the purpose of the assessment, the extent of the study area, and data availability (Aleotti et al. 1996), a medium scale (1:50,000) is chosen as the work scale to analyze landslide susceptibility zonation. Additionally, only a few landslide areas (about 0.05 % of the total landslide number) are less than 100 m<sup>2</sup> (Chong Xu et al. 2013), and 1:50,000 map scale is deemed sufficient to delineate a landslide.

In this study, a total of 4771 landslides are identified via RapidEye in 5 m resolution, SPOT-5 in 2.5 m resolution, IKONOS in 1 m resolution, and QuickBird in 0.6 m resolution, and about 80 % of these landslides are verified by field surveys; however, main scarps of landslides larger than one cell (25 × 25 m<sup>2</sup>) were selected in the landslide inventory mapping (the number adds up to 1773; Fig. 3). Most of the landslides were rock slides according to the classification system proposed by Varnes (1978). Among these data, a random 70 % of the data were chosen as training data for the landslide susceptibility map, while the remaining 30 % were used for the model validation. The pixel size of landslide inventory and other thematic maps was 25 m. The study area includes 2,264,362 pixels, and the main scarps of landslides include 63,631 pixels.

### Slope degree

The main parameter of the landslide stability analysis is the slope degree, since it dictates the distribution of slope stress (Lee and Min 2001; Saha et al. 2005; Ercanoglu et al. 2002). Meanwhile, the slope degree also restricts the redistribution of material and energy of the earth's surface and controls terrestrial plumbing, the thickness of the loose material, and recharge and discharge of groundwater on the slope. Most importantly, the slope influences the effective free face of the slope body, for landslides tend to increase with the free face of the slope body. For these reasons, the slope degree map of the study area is crucial for this research. The slope degree map is derived from DEM and divided into six slope categories (Fig. 4a).

### Aspect

Aspect is defined as the direction of the maximum slope of the terrain surface. It has an indirect influence on slope instability. Aspect related factors, such as exposure to sunlight, land use, drying winds, rainfall (degree of saturation), and discontinuities, may control the occurrence of landslides (Yalcin 2008). For example, Xu et al. (2013b)

has reported that large numbers of landslides caused by the Wenchuan earthquake occurred in south-facing aspects. Therefore, in this study, the aspect map is also derived from DEM and divided into nine classes: flat (−1°), north (337.5°–360°, 0°–22.5°), northeast (22.5°–67.5°), east (67.5°–112.5°), southeast (112.5°–157.5°), south (157.5°–202.5°), southwest (202.5°–247.5°), west (247.5°–292.5°), northwest (292.5°–337.5°) (Fig. 4b).

### Altitude

Altitude is also a relevant landslide conditioning factor. It is well known that altitude influences temperature, vegetable, human activity, and gravitational energy of landslides. In turn, these conditions have the potential to affect slope stability and generate slope failure. The altitude map is derived from DEM and reclassified into seven classes (Fig. 4c).

### Profile curvature

The profile curvature is theoretically defined as the rate of change of slope gradient or aspect, usually in one particular direction (Wilson and Gallant 2000). Profile curvature on the slope erosion processes influences the convergence or divergence of water during downhill flow (Ercanoglu and Gokceoglu 2002; Oh and Pradhan 2011). In addition, it also controls the change of velocity of mass flowing down the slope (Talebi et al. 2007). It is negative when the concavity of the normal section directed up and vice versa (Hengl et al. 2003). The profile curvature map was created by using a spatial geo-scientific analyses model in ArcGIS software (Fig. 4d).

### Geology and lithology

Geology and lithology describe the material basement of landslides. Rock types and structures decide the physical properties of rocks and thus affect the stability of landslides. For this reason, it is essential to group the lithology properties properly (Dai et al. 2001; Duman et al. 2006). In this study area, different lithology associations are developed in different geological periods (Table 2). The geological map was prepared by the Geological Survey of Sichuan province with 1:20,000 scale, then digitized and converted into raster format with 25-m pixel size in GIS (Fig. 4e).

### Distance from faults

The specific shape, type, and displacement mechanism of landslides were decided by pre-landslide geological features. Tectonic action plays important role in landslides

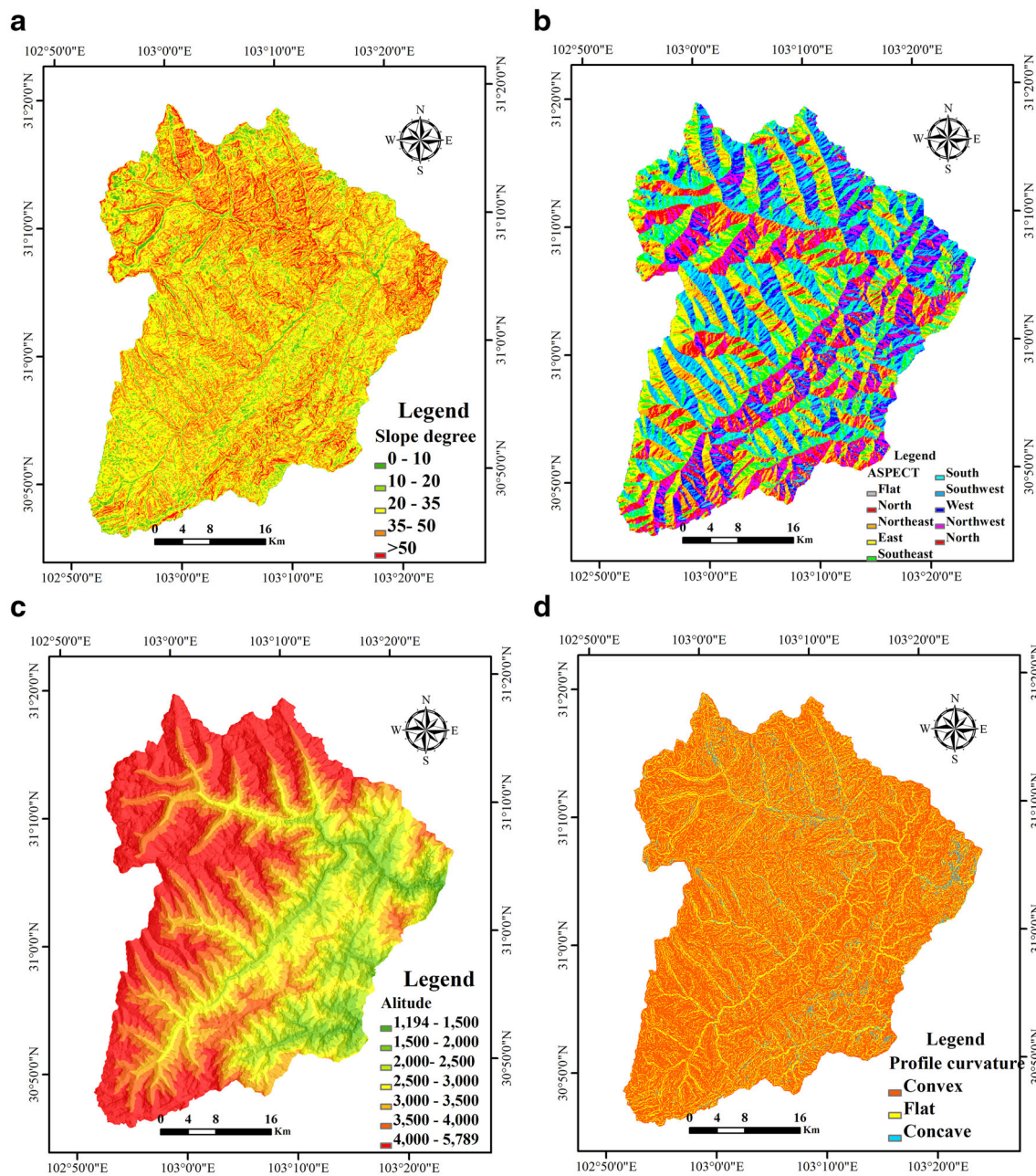


**Fig. 4** The thematic map of landslide affecting factor. **a** Slope degree; **b** aspect; **c** altitude; **d** profile curvature; **e** geology and lithology; **f** distance from faults; **g** distance from rivers; **h** distance from roads; **i** normalized difference vegetation index

occurrence. Faults form a line or zone of weakness characterized by tectonic structure (Foumelis et al. 2004). Generally speaking, landslides occur more frequently near the faults. Selective erosion and water movement along fault planes promote landsliding. In this study, the distance-from-faults map was extracted from the geology map at 1:200,000 scale. The buffer intervals were set to 200 m, and then the buffer map was converted into raster format (Fig. 4f).

#### Distance from rivers

The distance of the slope to drainage structure is another important factor in terms of landslide stability. Streams may adversely affect stability by eroding the slope or saturating the lower part of the material resulting in water level increases (Gokceoglu and Aksoy 1996; Saha et al. 2002). For this reason, six different buffer zones were defined with 100-m intervals to determine how the streams affected the slopes (Fig. 4g).

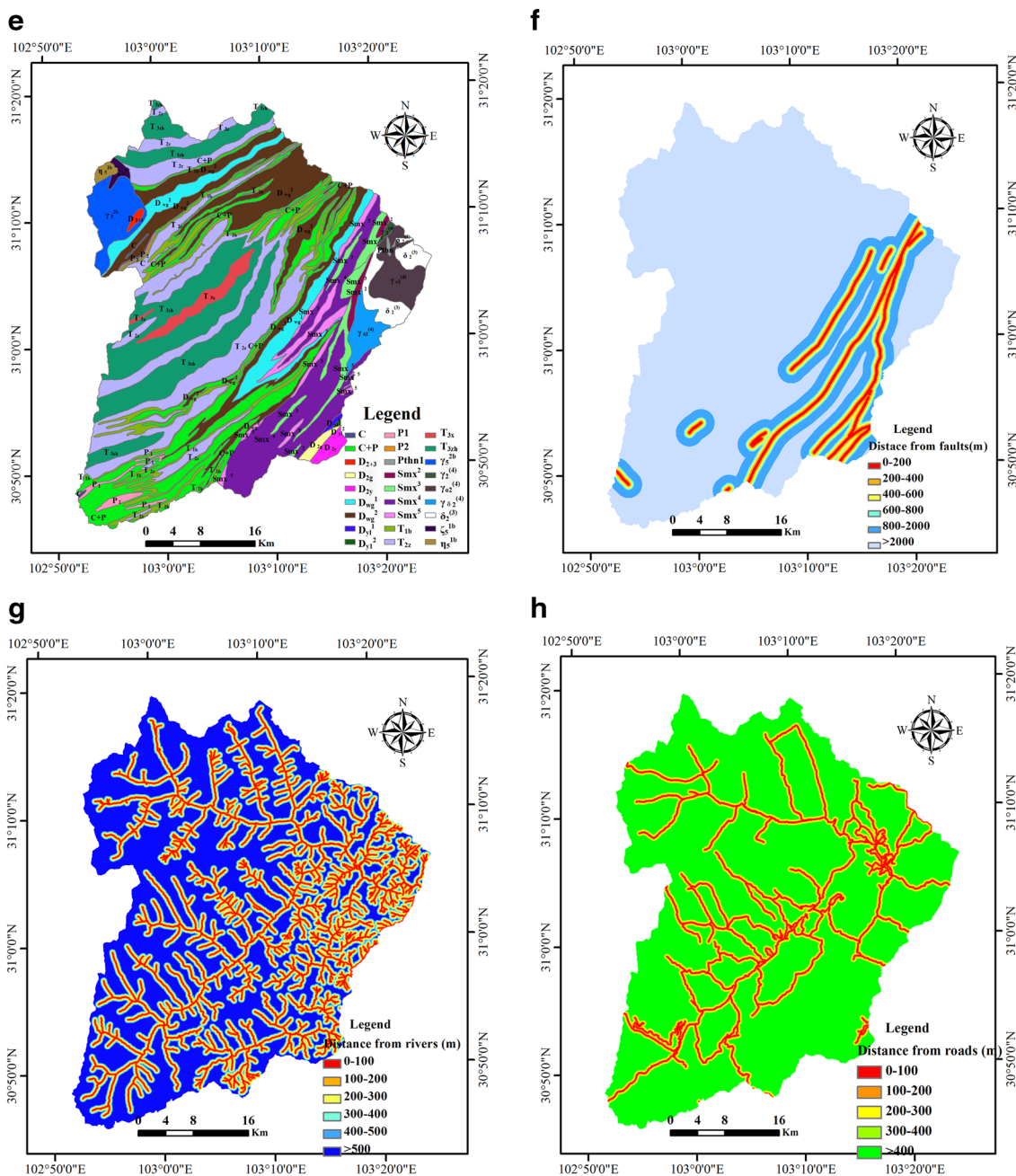


Fig. 4 continued

**Distance from roads**

Distance from roads is another important factor. A high slope caused by road excavation is more prone to slide owing to disruption of the stress state and slope equilibrium. In fact, a large number of landslides were observed closer to the road during the field investigation. For this reason, five different buffer zones were created with 100-m intervals to determine how the roads affected the stability of slope (Fig. 4h).

**Normalized difference vegetation index (NDVI)**

The incidence of landslides is closely related to vegetation density. Barren slopes are more prone to landslides as compared to one with higher vegetation coverage. The NDVI was derived from German remote sensing images (RapidEye) with 5 \* 5 m resolution. The NDVI value was calculated using the following equation:

$$NDVI = (NIR - R)/(NIR + R) \tag{1}$$



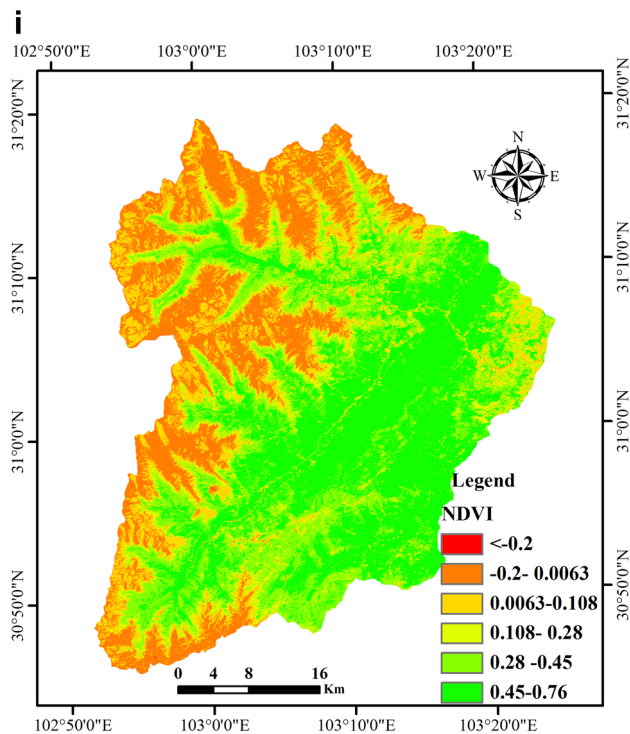


Fig. 4 continued

where NIR is the infrared value, and  $R$  is the red portion of the electromagnetic spectrum, respectively. The study area was divided into six classes to demonstrate how the NDVI influences landslide occurrence (Fig. 4i).

## Landslide susceptibility mapping

### Logistic regression model

Logistic regression (LR) is a multivariate analysis model used to find the optimal fitting to describe the relationship between the presence and absence of landslides based on a set of independent variables such as slope angle, aspect, and lithology. In the present situation, the dependent variable is a binary variable 0 or 1 that represents the absence or presence of a landslide. The LR model generates coefficients to estimate ratios for each of the independent variables.

Quantitatively, the relationship between occurrence and its dependency on several variables can be expressed as:

$$p = \frac{1}{1 + e^{-z}} \quad (2)$$

where the  $p$  value is the estimated probability of landslide occurrence, and  $Z$  is the linear combination of each affecting factor.

It follows that logistic regression involves fitting an equation of following form to the data

$$z = (b_0 + b_1x_1 + b_2x_2 + \dots + b_nx_n), \quad (3)$$

where  $b_0$  is the intercept of the model;  $b_i$  ( $i = 0, 1, 2, \dots, n$ ) is the partial regression coefficient;  $x_i$  ( $i = 0, 1, 2, \dots, n$ ) is the independent variable.

Before using the logistic regression model, the spatial databases of each factor influencing the landslide were converted to ASCII format files. Then, the coefficient between the landslide and each affecting factor was calculated by statistical software (SPSS 15.0).

$$\begin{aligned} z = & (0.12 \times \text{SLOPE}) + (0.178 \times \text{ASPECT}) \\ & + (0.058 \times \text{LITHOLOGY}) + (0.071 \times \text{NDVI}) \\ & + (0.012 \times \text{FAULT}) + (0.193 \times \text{ROAD}) \\ & + (0.064 \times \text{RIVER}) + (0.275 \times \text{ALTITUDE}) \\ & - (0.027 \times \text{Procur}) - 0.594 \end{aligned} \quad (4)$$

where SLOPE is slope value; ASPECT is aspect value; LITHOLOGY is geology and lithology value; NDVI is NDVI value; FAULT is distance from fault value; ROAD is distance from road value; RIVER is distance from river value; ALTITUDE is altitude value; Procur is profile curvature value; and  $z$  is a parameter.

Using Eqs. (2) and (3), the possibility of a landslide occurrence was calculated, and finally, a susceptibility map was obtained by converting the file into raster format. The  $p$  value ranges from 0.42 to 0.83. Five classes (very low, low, moderate, high, very high) were defined based on the standard deviation (Fig. 5a).

### Analytical hierarchy process (AHP)

The analytical hierarchy process, developed by Saaty (1977), is a semi-qualitative method based on pair-wise comparison of the contribution of different factors for landslide occurrence. It is a multi-objective, multi-criterion, decision-making approach that enables the user to arrive at scale of preference drawn from a set of alternatives (Saaty 1980). The decision maker can obtain the goal using the following steps:

1. Break down a complex and unstructured problem into component factors;
2. Arrange these factors in a hierarchical order;
3. Assign numerical values, weights, according to their subjective relevance to determine the relative importance of each factor;
4. Synthesize the judgments to determine the priorities of these factors (Saaty and Vargas 2001). In order to construct the pair-wise comparison matrix, each factor should be rated against any other factor by assigning a score between 1 and 9, given in Table 3.

**Table 2** Geology and lithology of the study area

Geological age	Lithology	Formation	Symbol
Indo-Chinese	Monzonite		$\eta_5^{1b}$
Indo-Chinese	Hatherlite porphyry		$\zeta_5^{1b}$
Yanshanian	Plagioclase granite		$\gamma_{\delta 2}^{(4)}$
Yanshanian	Porphyritic biotite granite		$\gamma_5^{2b}$
Proterozoic	Basalt, andesite, dacite, rhyolite with dacite	Huangshuihe	Pthn1
Proterozoic	Granodiorite	–	$\gamma_{\delta 2}^{(4)}$
Proterozoic	Diorite	–	$\delta_2^{(3)}$
Proterozoic	Biotite granite		$\gamma_2^{(4)}$
Silurian	Celadon phyllite, quartzite	Dier	Smx <sup>2</sup>
Silurian	Dark grey phyllite includes crystalline limestone, sandstone, dolomite	Disan	Smx <sup>3</sup>
Silurian	Schist, killas	Maoxian	Smx <sup>4</sup>
Silurian	Celadon phyllite and grey phyllite, crystalline limestone	Diwu	Smx <sup>5</sup>
Devonian	Phyllite and limestone, quartzite	Yuelizhai	D <sub>y1</sub> <sup>1</sup>
Devonian	Phyllite, limestone	Yuelizhai	D <sub>y1</sub> <sup>2</sup>
Devonian	Marlstone includes sandstone	Yangmaba	D <sub>2y</sub>
Devonian	Dolomitic limestone, dolomite and a little shale	Guanwushan	D <sub>2g</sub>
Devonian	Phyllite includes limestone, crystalline limestone	Weiguan	D <sub>wg</sub> <sup>1</sup>
Devonian	Phyllite, quartzite		Dwg <sup>2</sup>
Devonian	Phyllite, quartzite, and a little crystalline limestone		D <sub>2+3</sub>
Permian	Basalt, psephitic limestone, limestone		P
Permian	Limestone, dolomite limestone with intercalations of chert limestone		P <sub>1</sub>
Permian	Marlstone, chert limestone, shale with intercalations of bauxite and coal bed		P <sub>2</sub>
Triassic	Phyllite includes limestone, fine sandstone, and siltstone	Xikang	T <sub>1b</sub>
Triassic	Limestone, metamorphic quartz sandstone, and a little phyllite	Xikang	T <sub>2z</sub>
Triassic	Fine sandstone and siltstone, phyllite and a little limestone	Xindu	T <sub>3zh</sub>

When the factor on the vertical axis is more important than the factor on the horizontal axis, this value varies between 1 and 9. Conversely, the value varies between the reciprocal 1/2 and 1/9. According to the above principles, the importance of each parameter affecting landslide susceptibility and a calculated consistency ratio (CR) were generated (Table 4). In the AHP method, the CR is used to indicate the probability that the matrix judgments were randomly generated. When CR is less than 0.1, it represents a reasonable level of consistency (Malczewski 1999).

On the contrary, the judgment is needed when the CR is above 0.1. In this study, the CR is 0.0551, which means the ratio indicates a reasonable level of consistency in the pairwise comparison matrix. Geology and lithology, slope degree, distance from faults, and NDVI were found to be important parameters influencing the landslide occurrence, whereas distance from river is of low importance. Using a weighted linear sum procedure, the acquired weights were used to calculate the landslide susceptibility models.

$$LSM_{AHP} = \sum R_{li} \cdot W_{li} \quad (5)$$

where  $R_{li}$  is the rating class of each layer such as slope, aspect, elevation, where  $W_{li}$  is the weight for each conditioning factor. Based on the GIS, each conditioning factor is converted into raster format and weighted summation. The pixel values obtained are then classified into five classes based on standard deviation to determine the class intervals in the landslide susceptibility map (Fig. 5b).

### Combined SVM and fuzzy similarity model

The novel hybrid learning model is the combination of SVM and fuzzy similarity concept. Fuzzy similarity is attractive because it is straightforward to understand and implement. It is different from data-driven approaches such as logistic regression or weight of confidence (Pradhan 2011a, b). However, the weight of thematic layer in the fuzzy similarity method is controlled by the expert; in other words, the determination of weights is qualitative not quantitative. Consequently, combined fuzzy similarity with SVM can integrate advantages of two methods and provide objective and steady results. The flow diagram in Fig. 6

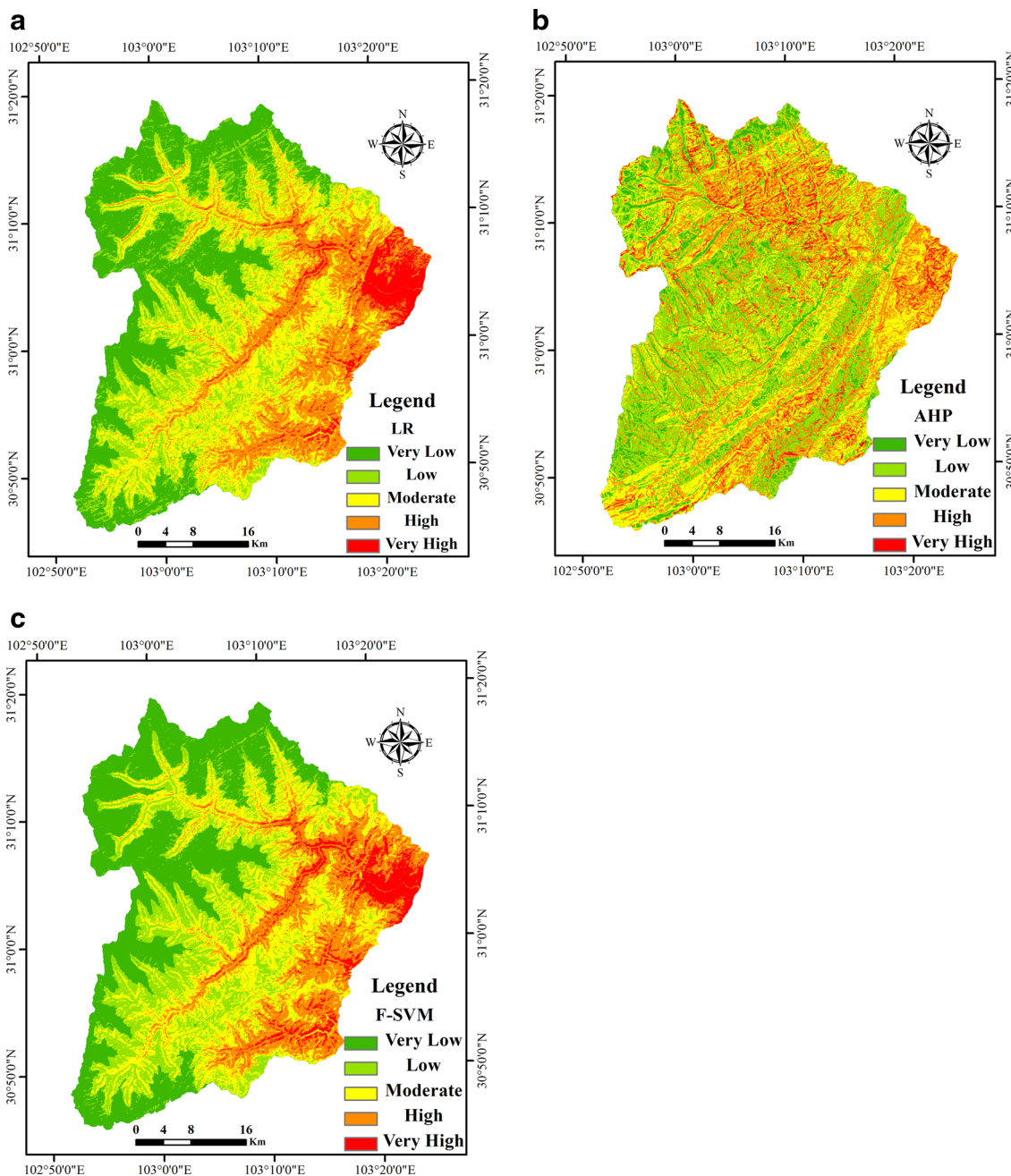


**Fig. 5** Landslide susceptibility map using LR model (a); AHP model (b); F-SVM (c)

involves three steps. Firstly, determine the rates of thematic layers using the fuzzy similarity approach. Secondly, determine the weights of thematic layers through the SVM approach. Finally, integrate the weights and rates using GIS to generate landslide susceptibility mapping. The flow diagram of this hybrid method is shown in Fig. 6.

#### *Fuzzy similarity method*

To deal with complex problems, Zadeh (1965) first introduced fuzzy set theory, which was oriented to the rationality

of uncertainty due to imprecision or vagueness. In fuzzy similarity theory, a spatial object is a member of set. Such a set is characterized by a membership, which can be assigned any value between 0 and 1, reflecting the degree of certainty of membership (Zadeh 1965). If the object belongs to member of set, the value is 1, otherwise the value is 0.

In this study, the membership degrees of categories of each conditioning factor are determined based on a frequency ratio model. The frequency ratio is the ratio of area where landslides occurred in the total area. If the value is greater than 1, it shows that this affecting factor has a high

**Table 3** Scale of preference between two parameters in AHP (Satty 2000)

Scales	Explanation
1	Equal importance
3	Moderate prevalence of one over another
5	Strong or essential prevalence
7	Very strong or demonstrated prevalence
9	Extremely high prevalence
2, 4, 6, 8	Intermediate values
Reciprocals	For inverse comparison

correlation with landslide occurrence; if lower than 1, it is a lower correlation; if equal to 1, it means an average value. Then, the frequency ratio normalized between 0 and 1 to describe the fuzzy membership values (Table 5).

### Support vector machines

The support vector machine was originally developed by Vapnik (1995) as a more recent machine-learning method after artificial neural networks.

Using the training data, SVM implicitly converts the original input space into higher dimensional feature space based on kernel functions (Brenning 2005). Subsequently, in the feature space, the optimal hyper-plane is determined by maximizing the margins of class boundaries (Shigeo Abe 2010). Therefore, SVM trains are modeled by constraining duality optimal solution.

Consider a training dataset of instance-label pairs  $(x_i, y_i)$ , with  $x_i \in R^n$ . The training vectors consist of two classes, which are denoted as  $y_i \in \{1, -1\}$  and  $i = 1, 2, \dots, m$ . If a point  $x_i \in R^n$  is above the hyper-plane, it is classified as 1, otherwise it is  $-1$ . The goal of SVM is to search for an  $n$ -dimensional hyper-plane differentiating the two classes by the maximum gap.

Mathematically, it can be denoted as

$$\min \frac{1}{2} \|w\|^2 \quad (6)$$

Subject to the following constraints

$$y_i((w \cdot x_i) + b) \geq 1 \quad (7)$$

where  $\|w\|$  is the normal of the hyper-plane,  $b$  is a scalar base, and  $\cdot$  denotes the scalar product operation.

Introducing the Lagrangian multiplier, the cost function can be defined as

$$L = \frac{1}{2} \|w\|^2 - \sum_{i=1}^n \lambda_i (y_i((w \cdot x_i) + b) - 1), \quad (8)$$

where  $\lambda_i$  is the Lagrangian multiplier. The solution can be achieved by dually minimizing Eq. (8).

For the case of linear separable data, a separate hyper-plane can be defined as

$$y_i((w \cdot x_i) + b) \geq 1 - \xi_i, \xi_i \geq 0, \quad (9)$$

where  $\xi_i$  is the slack variable. The above equation will be modified as

$$L = \frac{1}{2} \|w\|^2 - \frac{1}{\nu n} \sum_{i=1}^n \xi_i, \quad (10)$$

where  $\nu(0,1]$  is introduced to account for misclassification (Scholkopf et al. 2000; Hastie et al. 2001). Additionally, a kernel function  $K(x_i, y_i)$  is introduced accounting for the nonlinear decision boundary.

$$K(x_i, x_j) = e^{-\gamma(x_i - x_j)^2} \quad (11)$$

Generally speaking, there are several kernel types, such as linear kernel, polynomial kernel, RBF (Gaussian kernel). Because the RBF kernel has proved to be the most powerful kernel in dealing with nonlinear cases (Yao et al. 2008) it was thus employed in this study. For the RBF kernel, the kernel width ( $\gamma$ ) is the primary parameter, which controls the degree of nonlinearity of the SVM model (Damasevicius 2010). Only ( $\gamma$ ) has to be determined for a chosen  $\nu$ . For each pair ( $\gamma, \nu$ ), the dataset is divided into  $n$  folds: one fold is considered as verification dataset, the other  $n - 1$  folds are considered as training datasets. By iterating each fold as a verification dataset and combination of other folds as training, the optimal ( $\gamma, \nu$ ) is determined. For this research, ( $\gamma, \nu$ ) is chosen to be (0.1, 0.65) based on a 60 % subset of test data as training data and the other 40 % of the data as verification data. Final weights of landslide conditioning factors are given in Table 6 using the SVM model. Datasets and their classes are given in Table 5. Landslide susceptibility map produced by SVM is shown in Fig. 5c.

It can be observed from Table 5 that when the slope degree is greater than 50, the frequency ratio value is 2.21. This means a high probability for landslide occurrence, and thus the corresponding value of fuzzy membership is 1. For slope degree between 0 to 10, the frequency ratio value is 0.3517, which indicates a low probability of landslide occurrence, and the corresponding value of fuzzy membership is 0. In terms of slope aspect, landslides were the most abundant on the southeast and south slopes. Thus, the hill slope facing the southeast or south is more susceptible to landslide. The slopes facing flat and northeast have a lower probability of landslide. With respect to the altitude, landslides were the most abundant on 1179–1500, 1500–2000, 2000–2500 m (1.88, 2.4837, and 2.094, respectively). In the case of geology and lithology, the frequency ratio (13.47) is the highest in the areas that are composed of plagioclase granite in Yanshanian period, and

**Table 4** The pair-wise comparison matrix, factor weights, and consistency ratio of the data layers

Factors	Classes	1	2	3	4	5	6	7	8	9	Rating ( $R_{1i}$ )
Slope (°)	0–10	1	3	4	6	8					0.0377
	10–20		1	2	6	8					0.0672
	20–35			1	2	4					0.1343
	35–50				1	3					0.2536
	>50										0.5072
Consistency ratio	0.0436										
Aspect	Flat	1	1/6	1/3	1/4	1/4	1/7	1/2	1/5	1/3	0.0017
	North		1	3	2	2	1/3	3	2	3	0.0111
	Northeast			1	1/2	2	1/4	2	1/2	1	0.004
	East				1	1/2	1/3	3	2	1/3	0.0066
	Southeast					1	1/4	2	1	2	0.0029
	South						1	2	4	3	0.0181
	Southwest							1	3	2	0.0029
	West								1	1/2	0.0079
	Northwest									1	0.0041
Consistency ratio	0.0228										
Elevation (m)	1179–1500	1	1	2	3	4	6	8			0.0075
	1500–2000		1	2	2	4	6	7			0.007
	2000–2500			1	2	3	5	7			0.0048
	2500–3000				1	2	5	7			0.0035
	3000–3500					1	3	6			0.0022
	3500–4000						1	3			0.001
	4000–5789							1			0.0006
Consistency ratio	0.0361										
Profile curvature	Concave	1	1/3	2							0.0108
	Convex		1	7							0.034
	Flat			1							0.0051
Consistency ratio	0.0025										
Distance from faults (m)	0–200	1	2	3	4	5	6				0.0524
	200–400		1	2	3	4	5				0.034
	400–600			1	2	3	4				0.0221
	600–800				1	2	3				0.0146
	800–2000					1	3				0.0093
	>2000						1				0.0054
Consistency ratio	0.0246										
Distance from river (m)	0–100	1	2	3	4	5	6				0.0098
	100–200		1	2	3	4	5				0.0065
	200–300			1	2	3	4				0.0041
	300–400				1	2	3				0.0026
	400–500					1	2				0.0017
	>500						1				0.0011
Consistency ratio	0.0194										
Distance from road (m)	0–100	1	2	3	4	5					0.0194
	100–200		1	2	3	4					0.0122
	200–300			1	2	3					0.0074
	300–400				1	3					0.0049
	>400					1					0.0026
Consistency ratio	0.0283										

**Table 4** continued

Factors	Classes	1	2	3	4	5	6	7	8	9	Rating ( $R_{1i}$ )
NDVI	-0.2 to 0.063	1	1/2	1/3	1	3					0.0164
	-0.063 to 0.108		1	1/2	2	3					0.0269
	0.108–0.28			1	2	3					0.0385
	0.28–0.45				1	2					0.0164
	0.45–0.76					1					0.0085
Consistency ratio	0.0291										
Geology and lithology	Indo-Chinese	1	2	1	3	2	2	2			0.0789
	Yanshanian		1	1	4	3	2	2			0.0714
	Proterozoic			1	2	2	4	3			0.0789
	Silurian				1	1/2	1/2	1/3			0.0305
	Devonian					1	3	2			0.0332
	Permian						1	2			0.0372
	Triassic							1			0.0236
Consistency ratio	0.0747										
Data layer											Weight ( $W_{ii}$ )
	Slope	1	6	5	1/4	7	3	2	2	5	0.1894
	Aspect		1	2	1/8	4	2	1/2	1/2	2	0.0634
	Elevation			1	1/6	1/2	1/3	1/5	1/4	1/2	0.0267
	Geology and lithology				1	9	6	4	3	7	0.3538
	Distance from river					1	1/3	1/6	1/3	1/3	0.0257
	Distance from road						1	1/4	1/3	1/2	0.0466
	Distance from fault							1	2	3	0.1378
	NDVI								1	3	0.1067
	Profile curvature									1	0.0498
Consistency ratio	0.0551										

few landslides are distributed in *C*, *T3zh*, *P1*, *P2*,  $\eta 51b$ ,  $\zeta 5^{1b}$ ,  $D_{2+3}$ ,  $\gamma 5^{2b}$ . In the case of profile curvature, the frequency ratio values were higher in concave areas and lower in flat areas. In the case of NDVI, the frequency ratio is higher in 0.063–0.108, 0.108–0.28, 0.28–0.45. In the case of distance from fault, at distances of 0–200, 200–400, 400–600, 600–800, 800–2000 m, the frequency ratios are 0.59, 0.739, 0.662, 1.154, 1.396, respectively, showing a high probability of landslide occurrence. In the case of distance from river, distances of 200–300, 300–400, and 400–500 m have a high probability for landslide. For the distance from the road, the landslides mostly occurred at distances of 100–200, 200–300, 300–400, >400 m.

## Results and comparison of multi-models

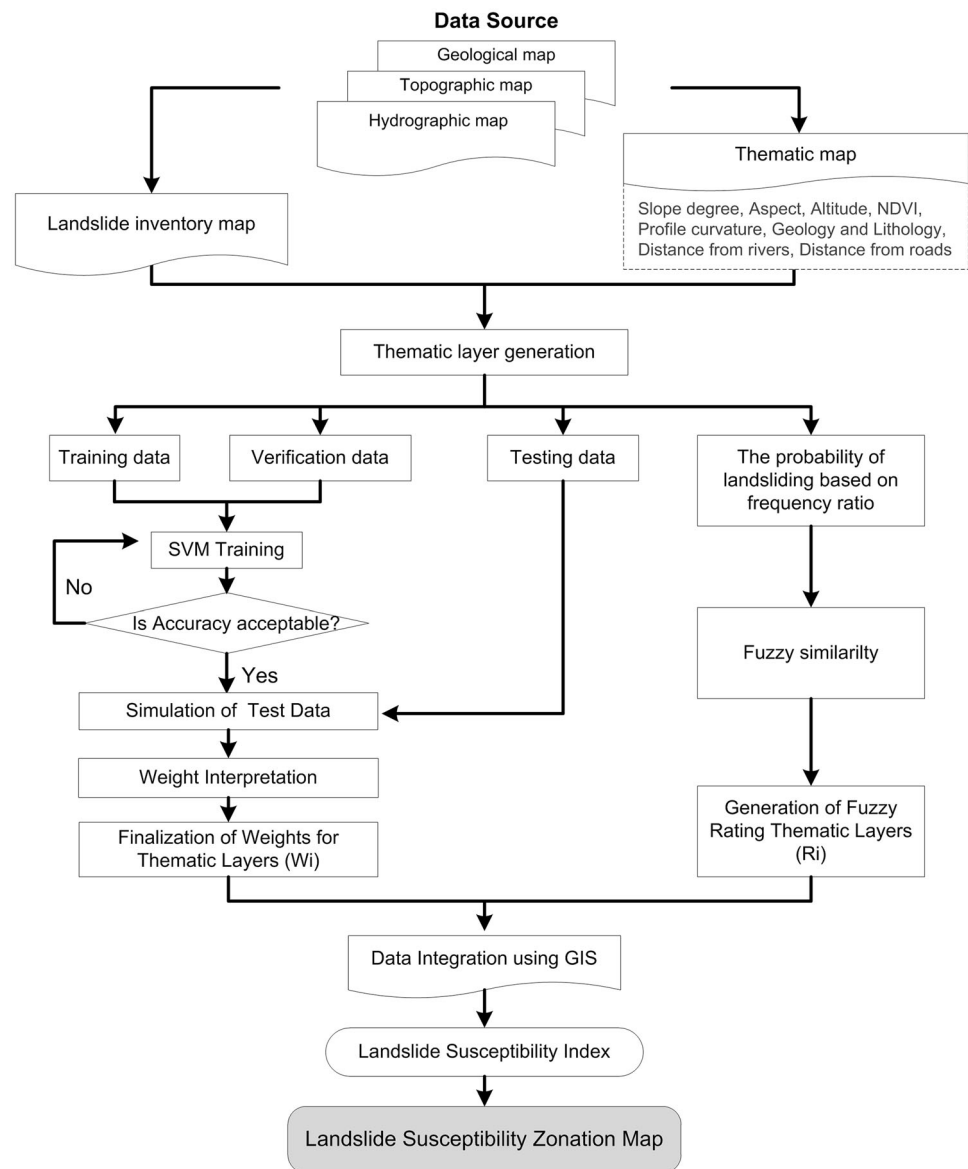
The LSZ was generated by three different methods based on GIS. To test the optimal approach, LR, AHP, and F-SVM were compared and validated. The percentage distribution of the susceptibility classes in the study area was determined by standard deviation classification, since

the histogram of data values exhibits a normal distribution.

According to the LSZ produced by the LR method, it can be observed that 5.34, 20.15, 29.0, 20.17, and 25.34 % of the study area can be classified as very high, high, moderate, very low, and low susceptibilities (Fig. 7). As shown in Fig. 7, the histogram of the landslide susceptibility area based on the AHP model exhibits that 9.8 % of the total area is very low probability for landsliding, and 5.4 % of the total area shows very high probability for landsliding. The low area covers about 30.9 % of the total area. The moderate susceptibility zone is about 27.6 % and the high susceptibility area is 26.1 %. According to the landslide susceptibility zone produced by F-SVM, 5.8 % of the study area is very high zonation, 17.8 % high, 26.7 % moderate, 21.1 % low, and 28.6 % very low area (Fig. 7).

For validation of landslide hazard calculation models, two assumptions are needed. One is that the landslides are related to spatial information. The other assumption is that future landslides will be triggered by specific factors such as rainfall and earthquake. In this study, both of the basic assumptions were met. The landslide susceptibility maps

**Fig. 6** Flow diagram showing the combined fuzzy and SVM method for landslide susceptibility mapping



can be validated by comparing the known landslides location data, which were not included in the susceptibility analyses, with the susceptibility map obtained. In the present study, 30 % of total landslides were used for validation based on random selection. Figure 8 presents a histogram that summarizes the results of the entire process. It can be observed that 41.7, 40.9, 13.6, 3.6 % of the validation hazard data fall into the very high, high, moderate, and low classes of the landslide susceptibility map using the F-SVM method. Of the landslides that occurred, 38.7, 41.3, 15.8, and 4 % fall into the very high, high, moderate, and low susceptibility classes in LSZ with the LR method. It is worth mention that no validation data falls into the very low susceptible class in LSZ with F-SVM and LR. The landslide susceptibility map created with the AHP method showed that 10, 51.2, 26.5, 10.7, 1.4 % of

landslides that occurred fall into very high, high, moderate, low, very low susceptible classes.

Moreover, the rate curves are generated, and the area under curve (AUC) is a good indicator to evaluate the prediction performance of the model. If the AUC is close to 1, it indicates a more ideal model (Swets 1988; Yesilnacar and Topal 2005). To obtain the relative ranks for each prediction model, the calculated landslide susceptibility index (LSI) of all cells in the study area was sorted in descending order. Then the ordered cell values were divided into 100 classes with accumulated 1 % intervals. Cumulative percentage of landslide occurrence in different models appears as a line in Fig. 9. It can be observed from Fig. 9 that three different methods show the same tendency. This means all three methods can be used for predicting the susceptibility of landslide. In the case of the

**Table 5** Spatial probability relationship between each landslide affecting factor and landslide and fuzzy membership value

Factor	Class	Percentage of domain (%)	Percentage of landslides (%)	Frequency ratio	Fuzzy membership value ( $R_i$ )
Slope	0°–10°	7.3	2.56	0.3517	0
	10°–20°	15.81	9.37	0.5925	0.13
	20°–35°	42.08	33.27	0.79	0.23
	35°–50°	29.36	42.7	1.45	0.59
	>50°	5.43	12.02	2.21	1
Aspect	Flat	0.00001	0	0	0
	North	11.7	10.8	0.859	0.57
	Northeast	11.8	5.98	0.5064	0.34
	East	15.5	12.43	0.798	0.53
	Southeast	14.20	21.1	1.4853	1
	South	12.35	16.8	1.364	0.91
	Southwest	12.63	11.06	0.875	0.589
	West	10.48	8.4	0.808	0.54
	Northwest	11.17	13.96	1.248	0.84
Altitude (m)	1179–1500	0.319	0.6	1.880	0.75
	1500–2000	5.02	12.4	2.483	1
	2000–2500	12.45	26.0	2.094	0.84
	2500–3000	16.27	24.3	1.497	0.59
	3000–3500	17.11	18.3	1.069	0.423
	3500–4000	18.51	17.1	0.926	0.36
	4000–5789	30.29	0.98	0.0324	0
Distance from river (m)	0–100	13.9	8.0	0.575	0
	100–200	11.28	14.0	1.244	0.533
	200–300	11.6	19.4	1.674	0.877
	300–400	9.3	17.0	1.828	1
	400–500	9.19	13.4	1.468	0.712
	>500	44.6	27.9	0.626	0.04
Distance from fault (m)	0–200	2.88	1.72	0.59	0
	200–400	2.62	1.93	0.739	0.178
	400–600	2.64	1.74	0.662	0.082
	600–800	2.40	2.75	1.154	0.6973
	800–2000	12.32	17.2	1.396	1
	>2000	77.1	74.6	0.967	0.463
Distance from road (m)	0–100	6.13	5.8	0.956	0
	100–200	4.94	5.51	1.116	0.09
	200–300	5.10	7.45	1.460	1
	300–400	5.07	7.24	1.427	0.93
	>400	73.5	73.9	1.004	0.32
	Geology and lithology	$\eta_5^{1b}$	0.296	0	0
$\zeta_5^{1b}$		0.296	0	0	0
$\gamma_{o2}^{(4)}$		2.47	17.4	7.06	0.52
$\gamma_5^{2b}$		3.1	0	0	0
Pthn1		0.065	0.08	13.47	1
$\gamma_{82}^{(4)}$		1.56	6.33	4.057	0.3
$\delta_2^{(3)}$		2.13	12.9	6.051	0.448
$\gamma_2^{(4)}$		0.136	0.24	1.806	0.34
Smx <sup>2</sup>		0.494	0.40	0.829	0.06
Smx3		2.30	2.26	0.984	0.07



**Table 5** continued

Factor	Class	Percentage of domain (%)	Percentage of landslides (%)	Frequency ratio	Fuzzy membership value ( $R_i$ )
	Smx4	9.403	3.90	0.415	0.03
	Smx5	2.27	1.58	0.696	0.052
	$D_{y1}^1$	0.109	0.24	2.24	0.166
	$D_{y1}^2$	0.03	0.08	2.68	0.199
	$D_{2y}$	0.603	0.13	0.226	0.0167
	$D_{2g}$	0.386	0.6	1.554	0.115
	$D_{wg}^1$	4.831	2.97	0.616	0.045
	$Dwg^2$	12.92	13.5	1.046	0.077
	$D_{2+3}$	0.156	0	0	0
	P1	0.832	0	0	0
	P2	0.067	0	0	0
	T1b	6.52	9.0	1.39	0.1
	T2z	17.05	10.81	0.634	0.047
	T3zh	16.21	0.4	0.025	0.002
NDVI	< -0.2	0.018	0	0	0
	-0.2 to 0.063	19.8	11.6	0.585	0.224
	0.063 to 0.108	15.1	6.15	0.405	0.155
	0.108 to 0.28	9.9	25.8	2.610	1
	0.28 to 0.45	20.8	33.24	1.592	0.609
	0.45 to 0.76	34.2	23.15	0.6763	0.259
Profile curvature	Flat	80	61.4	0.767	0
	Convex	9.76	12.3	1.265	0.27
	Concave	10.22	26.2	2.564	1

**Table 6** Weights of each landslide affecting factor based on SVM model

Factor	Weight ( $W_i$ )
Slope	0.1991
Aspect	0.2408
Altitude	0.8213
NDVI	0.1417
Geology and lithology	0.5955
Distance from faults	0.0387
Distance from rivers	0.1056
Distance from roads	0.0721
Profile curvature	-0.0293
Constant	-0.2896

AHP method, 90 to 100 % (10 %) class of the study area where the landslide hazard index had a high rank could explain 40.22 % of all the landslides. Additionally, 80–100 % (20 %) class of the study area where the landslide hazard index had a high rank could explain 63.09 % of all the landslides. In the case of the LR approach, 90–100 % (10 %) class of the study area where the

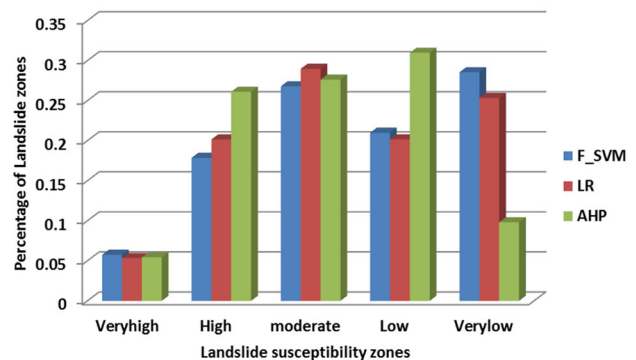


**Fig. 7** A histogram showing the percentage of landslide zones constructed with the LR, AHP, F-SVM methods

landslide hazard index had a high rank could explain 52.713 % of all the landslides. In addition, the 80–100 % (20 %) class of the study area where the landslide hazard index had a high rank could explain 71.98 % of all the landslides. In the case of the fuzzy-SVM method, 90–100 % (10 %) class of the study area where the landslide hazard index had a high rank could explain 53.13 % of all the landslides. In addition, 80–100 % (20 %) class of

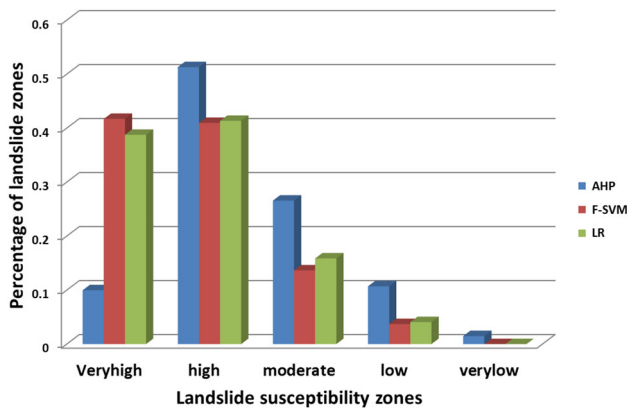


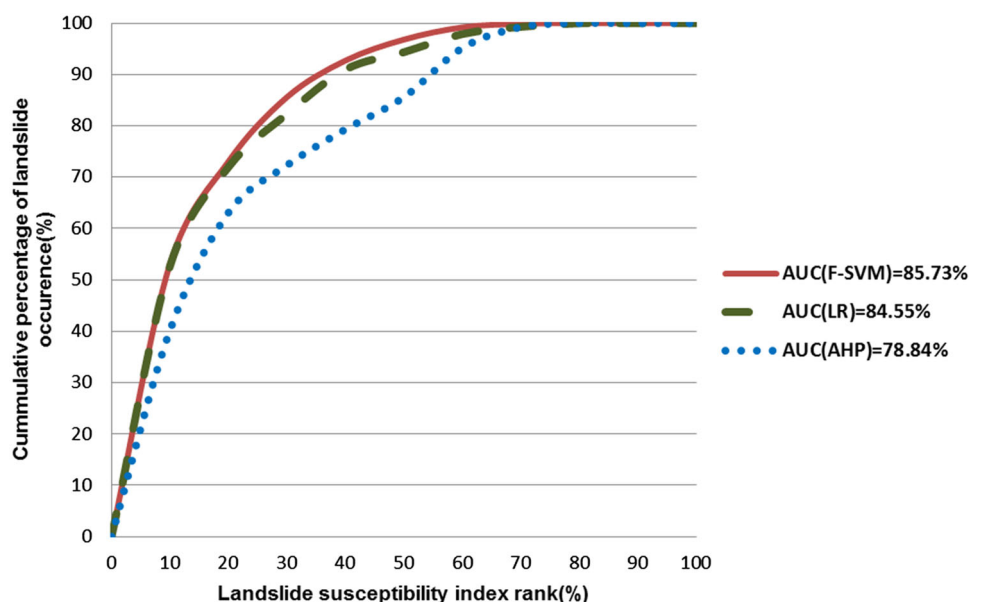
**Fig. 8** A histogram showing the verification data that fall into the various classes of the LR, AHP, F-SVM susceptibility maps

the study area where the landslide hazard index had a high rank could explain 73.06 % of all the landslides. In order to be compared with the prediction accuracy of different methods quantitatively, the area under the curve needs to be calculated. In the case of the AHP method, the area ratio was 0.7884. In other words, the prediction accuracy is 78.84 %. In the case of the LR method, the prediction accuracy is 84.55 %. In the case of the fuzzy-SVM method, the prediction accuracy is 85.73 %. It is easy to conclude that F-SVM has better prediction than AHP, whereas it is relatively similar to LR.

## Discussion and conclusions

Since landslides are among the most dangerous natural hazards, government and research institutions worldwide have attempted to assess landslide susceptibility, risk, and

**Fig. 9** Cumulative frequency diagram showing landslide hazard index rank occurring in cumulative percent of landslide occurrence



show its spatial distribution. The research for assessing hazard susceptibility in cultural heritage sites or natural heritage sites is relatively few (Kyoji Sassa et al. 2009). Wolong Giant Panda Natural Reserve, as one of the world's cultural heritages, is located southwest of the epicenter of the Wenchuan earthquake at a distance of about 30 km. Obviously, the Wenchuan earthquake had triggered enormous landslides and caused larger landslide susceptible areas. In the present study, a total of 1773 landslide scarps larger than one cell ( $25 \times 25 \text{ m}^2$ ) were selected in the landslide inventory mapping, 70 % of which are randomly selected to be used as test data, and the other 30 % are used as validation. Nine landslide conditioning factors were selected: slope degree, aspect, altitude, profile curvature, geology and lithology, distance from faults, distance from rivers, distance from roads, and normalized difference vegetation index (NDVI). The logistic regression, analytical hierarchy process, and combined fuzzy and SVM were applied and compared for landslide susceptibility mapping in Wolong Giant Panda Natural Reserve. The validation was carried out and showed that combined fuzzy and SVM hybrid model would be the most accurate LSZ map in this study area.

Many studies have compared neural network models with LR, AHP, and conditional probability. Some authors agree that soft computing (e.g., ANN, SVM) models have superior performance to conventional conditional probability or LR methods (Yao et al. 2008), while other authors find that soft computing models have no difference with other prediction methods (Tu 1996; Schumacher et al. 1996; Ottenbacher et al. 2001; Mahiny and Turner 2003).

In this study, our results demonstrate that although three different methods can predict landslide susceptibility

according to their same tendency, the combined fuzzy and SVM method (F-SVM) is better than AHP and has relative similar accuracy to LR. The AHP method is a simple tool and easy to be implemented based on expert opinion, but the limitation is results with uncertainty and subjectivity. The LR method is relatively excellent, for it can decrease the subjective result to some extent as a data-driven model. However, the combined fuzzy and SVM hybrid model performed the most excellent. This may be because SVM represents an objective approach, where weights for each landslide conditioning factor are determined through the SVM model, and rating of the thematic layer is determined by the fuzzy similarity method.

In summary, the landslide susceptibility map generated by the combined fuzzy and SVM hybrid model in Wolong Giant Panda Natural Reserve is the objective approach. According to LSZ based on F-SVM, 5.8, 17.8 % of the study area is assigned as very high and high susceptibility areas, which is very meaningful for government, managers, and decision makers of protecting giant panda.

**Acknowledgments** This research is supported by the Open Fund of the Center for Earth Observation and Digital Earth, the Chinese Academy of Sciences (grant No. 2013LDE006). We would like to thank Dr.s Xinyuan Wang, Chuan Sheng Liu, and Jing Zhen for providing various datasets and advice throughout this research.

## References

- Abe Shigeo (2010) Support vector machines for pattern classification. Springer, Berlin
- Akgun A, Türk N (2010) Landslide susceptibility mapping for Ayvalik (Western Turkey) and its vicinity by multi-criteria decision analysis. *Environ Earth Sci* 61:595–611
- Akgun A, Dag S, Bulut F (2008) Landslide susceptibility mapping for a landslide-prone area (Findikli, NE of Turkey) by likelihood-frequency ratio and weighted linear combination models. *Environ Geol* 54(6):1127–1143
- Akgun A, Kincal C, Pradhan B (2011) Application of remote sensing data and GIS for landslide risk assessment as an environmental threat to Izmir city (west turkey). *Environ Monit Assess* 184(9):5453–5470
- Akgun A, Sezer EA, Nefeslioglu HA, Gokceoglu C, Pradhan B (2012) An easy-to use MATLAB program (MamLand) for the assessment of landslide susceptibility using a Mamdani fuzzy algorithm. *Comput Geosci* 38(1):23–34
- Aleotti P, Chowdhury R (1999) Landslide hazard assessment: summary review and new perspectives. *Bull Eng Geol Environ* 58(1):21–44
- Aleotti P, Baldelli P, Polloni G (1996) Landsliding and flooding event triggered by heavy rains in the Tanaro basin (Italy). *Proc Int Congr Interpraevent* 1:435–446
- Ali Yalcin (2008) GIS-based landslide susceptibility mapping using analytical hierarchy process and bivariate statistics in Ardesen (Turkey): comparisons of results and confirmations. *Catena* 72(1):1–12. doi:10.1016/j.catena.2007.01.003
- Ayalew L, Yamagishi H (2005) The application of GIS-based logistic regression for landslide susceptibility mapping in the Kakuda-Yahiko Mountains, central Japan. *Geomorphology* 65:15–31
- Ayalew L, Yamagishi H, Ugawa N (2004) Landslide susceptibility mapping using GIS-based weighted linear combination, the case in Tsugawa area of Agano River, Niigata Prefecture. *Japan. Landslides* 1(1):73–81
- Bai S, Lü G, Wang J, Zhou P, Ding L (2010) GIS-based rare events logistic regression for landslide-susceptibility mapping of Lianyungang, China. *Environ Earth Sci* 62(1):139–149
- Brabb EE, Pampeyan EH, Bonilla M (1972) Landslide susceptibility in the San Mateo County, California. In: *Miscellaneous Field Studies*, map MF-360. USGS, Reston
- Brenning A (2005) Spatial prediction models for landslide hazards: review, comparison and evaluation. *Nat Hazards Earth Syst Sci* 5(6):853–862
- Bui DT, Lofman O, Revhaug I (2011) Landslide susceptibility analysis in the Hoa Binh province of Vietnam using statistical index and logistic regression. *Nat Hazards* 59:1413–1444. doi:10.1007/s11069-011-9844-2
- Can T, Nefeslioglu HA, Gokceoglu C, Snomez H, Duman TY (2005) Susceptibility assessment of shallow earth flows triggered by heavy rainfall at three sub catchments by logistic regression analyses. *Geomorphology* 72:250–271
- Carrara A (1983) Multivariate models for landslide hazard evaluation. *J Int Assoc Math Geol* 15(3):403–426
- Carrara A, Merenda L (1976) Landslide inventory in northern Calabria, southern Italy. *Geol Soc Am Bull* 87:1153–1162
- Chauhan S, Sharma M, Arora MK, Gupta NK (2010) Landslide susceptibility zonation through ratings derived from artificial neural network. *Int J Appl Earth Obs Geoinform* 12:340–350
- Chong Xu, Xiwei Xu, Dai Fuchu, Zhide Wu, He Honglin, Shi Feng, Xiyuan Wu, Suning Xu (2013) Application of an incomplete landslide inventory, logistic regression model and its validation for landslide susceptibility mapping related to the May 12 2008 Wenchuan earthquake of China. *Nat Hazards* 68:883–900
- Chung CF, Fabbri AG, van Westen CJ (1995) Multivariate regression analysis for landslide hazard zonation. *Geographical information systems in assessing natural hazards*. Springer, Netherlands
- Clerici A, Perego S, Tellini C, Vescovi P (2006) A GIS-based automated procedure for landslide susceptibility mapping by the conditional analysis method: the Baganza valley case study (Italian Northern Apennines). *Environ Geol* 50(7):941–961. doi:10.1007/s00254-006-0264-7
- Constantin M, Bednarik M, Jurchescu MC (2011) Landslide susceptibility assessment using the bivariate statistical analysis and the index of entropy in the Sibiciu Basin (Romania). *Environ Earth Sci* 63(2):397–406
- Corominas J, Westen CV, Frattini P (2014) Recommendations for the quantitative analysis of landslide risk. *Bull Eng Geol Environ* 73(2):209–263
- Dai FC, Lee CF (2002) Landslide characteristics and slope instability modeling using GIS, Lantau Island, Hong Kong. *Geomorphology* 42(1):213–228
- Dai FC, Lee CF (2003) A spatiotemporal probabilistic modeling of storm-induced shallow landsliding using aerial photographs and logistic regression. *Earth Surf Proc Land* 28(5):527–545. doi:10.1002/esp.456
- Dai FC, Lee CF, Li J, Xu ZW (2001) Assessment of landslide susceptibility on the natural terrain of Lantau Island. *Hong Kong. Environ Geol* 40(3):381–391. doi:10.1007/s002540000163
- Dai FC, Lee CF, Tham LG, Ng KC, Shum WL (2004) Logistic regression modelling of storm-induced shallow landsliding in time and space on natural terrain of Lantau Island. *Hong Kong. Bull Eng Geol Environ* 63(4):315–327. doi:10.1007/s10064-004-0245-6
- Damasevicius R (2010) Structural analysis of regulatory DNA sequences using grammar inference and support vector machine. *Neurocomputing* 73(4–6):633–638

- Duman TY, Can T, Gokceoglu C, Nefeslioglu HA, Sonmez H (2006) Application of logistic regression for landslides susceptibility zoning of Cekmece Area, Istanbul, Turkey. *Environ Geol* 51:241–256
- Ercanoglu M, Gokceoglu C (2002) Assessment of landslide susceptibility for a landslide-prone area (North of Yenice, NW Turkey) by fuzzy approach. *Environ Geol* 41:720–730
- Ercanoglu M, Gokceoglu C (2004) Use of fuzzy relations to produce landslide susceptibility map of a landslide prone area (West Black Sea Region, Turkey). *Eng Geol* 75:229–250
- Ercanoglu M, Kasmer O, Temiz N (2008) Adaptation and comparison of expert opinion to analytical hierarchy process for landslide susceptibility mapping. *Bull Eng Geol Environ* 67:565–578
- Felicísimo A, Cuartero A, Remondo J, Quiros E (2013) Mapping landslide susceptibility with logistic regression, multiple adaptive regression splines, classification and regression trees, and maximum entropy methods: a comparative study. *Landslides* 10:175–189. doi:10.1007/s10346-012-0320-1
- Fenti V, Silvano S, Spagna V (1979) Methodological proposal for an engineering geomorphological map. Forecasting rockfalls in the alps. *Bull Eng Geol Environ* 19(1):134–138
- Foumelis M, Lekkas E, Parcharidis I (2004) Landslide susceptibility mapping by GIS- based qualitative weighting procedure in Corinth area. *Bull Geol Soc Greece* 36:904–912
- Goesevski PV, Gessler PE, Foltz RB, Elliot WJ (2006) Spatial prediction of landslide hazard using logistic regression and ROC analysis. *Trans GIS* 10(3):395–415
- Gokceoglu C, Aksoy H (1996) Landslides susceptibility mapping of the slopes in the residual soils of the Mengen region (Turkey) by deterministic stability analyses and image processing techniques. *Eng Geol* 44:147–161
- Guzzetti F, Carrara A, Cardinali M, Reichenbach P (1999) Landslide hazard evaluation: a review of current techniques and their application in a multiscale study, Central Italy. *Geomorphology* 31:81–216
- Hastie T, Tibshirani R, Friedman JH (2001) *The elements of statistical learning: data mining inference and prediction*. Springer, Berlin
- Hengl T, Gruber S, Shrestha DP (2003) *Digital terrain analysis in ILWIS*. International Institute for Geo-information Science and Earth Observation Enschede, The Netherlands
- Holec J, Bednarik M, Sabo M, Minar J, Yilmaz I, Marschalko M (2013) A small-scale landslide susceptibility assessment for the territory of Western Carpathians. *Nat Hazards* 69(1):1081–1107
- Ives JD, Messerli B (1981) Mountain hazard mapping in Nepal: introduction to an applied mountain research project. *Mt Res Dev* 3–4:223–230
- Kanungo DP, Arora MK, Sarkar S, Gupta RP (2006) A comparative study of conventional ANN black box, fuzzy and combined neural and fuzzy weighting procedures for landslide susceptibility zonation in Darjeeling Himalayas. *Eng Geol* 85:347–366
- Kayastha P, Dhital MR, De Smedt F (2013) Application of the analytical hierarchy process (AHP) for landslide susceptibility mapping: a case study from the Tinau watershed, west Nepal. *Comput Geosci* 52(1):398–408
- Kienholz H (1978) Maps of geomorphology and natural hazard of Griendelwald, Switzerland, scale 1:10.000. *Artic and Alpine Res* 10:169–184
- Kincal C, Akgun A, Koca MY (2009) Landslide susceptibility assessment in the Izmir (West Anatolia, Turkey) city center and its near vicinity by the logistic regression method. *Environ Earth Sci* 59:745–756
- Komac M (2006) A landslide susceptibility model using the analytical hierarchy process method and multivariate statistics in perialpine Slovenia. *Geomorphology* 74(1):17–28
- Lee S, Evangelista DG (2006) Earthquake-induced landslide-susceptibility mapping using an artificial neural network. *Nat Hazards Earth Syst Sci* 6:687–695
- Lee S, Min K (2001) Statistical analysis of landslides susceptibility at Yongin, Korea. *Environ Geol* 40(9):1095–1113
- Lee S, Min K (2004) Probabilistic landslide hazard mapping using GIS and remote sensing data at Boun, Korea. *International Journal of Remote Sensing* 25(11):2037–2052
- Lee S, Pradhan B (2007) Landslide hazard mapping at Selangor, Malaysia using frequency ratio and logistic regression models. *Landslides* 4(1):33–41
- Lee S, Choi J, Oh H (2009) Landslide susceptibility mapping using a neuro-fuzzy. *AGU Fall Meeting Abstracts #NH53A-1075*
- Lei TC, Wan T, Chou TY (2011) The knowledge expression on debris flow potential analysis through PCA + LDA and rough sets theory: a case study of Chen-Yu-Lan watershed, Nantou, Taiwan. *Environ Earth Sci* 63(5):981–997
- Lucà F, Conforti M, Robustelli G (2011) Comparison of GIS-based gully susceptibility mapping using bivariate and multivariate statistics: Northern Calabria, South Italy. *Geomorphology* 134(3):297–308
- Luzi L, Pergalani F, Terlien MT (2000) Slope vulnerability to earthquakes at subregional scale, using probabilistic techniques and geographic information systems. *Eng Geol* 58(3):313–336
- Magliulo P, Lisio AD, Russo F (2008) Geomorphology and landslide susceptibility assessment using GIS and bivariate statistics: a case study in southern Italy. *Nat Hazards* 47(3):411–435
- Mahiny AS, Turner BJ (2003) Modelling past vegetation change through remote sensing and GIS: a comparison of neural networks and logistics regression methods. *International conference on geoinformatics and modeling geographical system and fifth international workshop on Gis Beijing*, pp 2–4
- Malczewski J (1999) *GIS and multicriteria decision analysis*. Wiley, New York
- Micheletti N, Kanevski M, Bai SB, Wang J, Hong T (2013) Intelligent analysis of landslide data using machine learning algorithms. *Landslide Sci Pract* 3:161–167
- Mohammady M, Pourghasemi HR, Pradhan B (2012) Landslide susceptibility mapping at Golestan Province Iran: a comparison between frequency ratio, Dempster-Shafer, and weights-of-evidence models. *J Asian Earth Sci* 61:221–236
- Nandi A, Shakoor A (2010) A GIS based landslide susceptibility evaluation using bivariate and multivariate statistical analyses. *Eng Geol* 110(1):11–20
- Nefeslioglu HA, Duman TY, Duemaz S (2008a) Landslide susceptibility mapping for a part of tectonic Kelkit Valley (Eastern Black Sea region of Turkey). *Geomorphology* 94:401–418
- Nefeslioglu HA, Gokceoglu C, Sonmez H (2008b) An assessment on use of logistic regression and artificial neural networks with different sampling strategies for the preparation of landslide susceptibility maps. *Eng Geol* 97(3–4):171–191
- Oh HJ, Lee S (2010) Cross-validation of logistic regression model for landslide susceptibility mapping at Ganeoung areas, Korea. *Disaster Adv* 3(2):44–55
- Oh HJ, Lee S (2011) Cross-application used to validate landslide susceptibility maps using a probabilistic model from Korea. *Environ Earth Sci* 64(2):395–409
- Oh HJ, Pradhan B (2011) Application of a neuro-fuzzy model to landslide-susceptibility mapping for shallow landslides in a tropical hilly area. *Comput Geosci* 37(9):1264–1276
- Ottensbacher KJ, Smith PM, Illig SB, Linn RT, Fieldler RC, Granger CV (2001) Comparison of logistic regression and neural networks to predict hospitalization in patients with stroke. *Clin Epidemiol* 54:1159–1165

- Ouyang ZY, Xu WH, Wang XZ (2008) Impact assessment of Wenchuan earthquake on ecosystems. *Acta Ecol Sinica* 28:5801–5809
- Ozdemir A (2009) Landslide susceptibility mapping of vicinity of Yaka landslide (Gelendost, Turkey) using conditional probability approach in GIS. *Environ Geol* 57:1675–1686
- Piegari E, Cataudella V, Di Maio R, Milano L, Nicodemi M, Soldovieri MG (2009) Electrical resistivity tomography and statistical analysis in landslide modelling: a conceptual approach. *J Appl Geophys* 68(2):151–158
- Polykretis C, Ferentinou M, Chalkias C (2015) A comparative study of landslide susceptibility mapping using landslide susceptibility index and artificial neural networks in the Krios River and Krathis River catchments (northern Peloponnesus, Greece). *Bull eng geol environ* 74(1):27–45
- Pourghasemi HR, Pradhan B, Gokceoglu C, Mohammadi M, Moradi HR (2012a) Application of weights-of-evidence and certainty factor models and their comparison in landslide susceptibility mapping at Haraz watershed, Iran. *Arab J Geosci* 6(7):2351–2365
- Pourghasemi HR, Pradhan B, Gokceoglu C, Deylami Moezzi K (2012b) A comparative assessment of prediction capabilities of Dempster-Shafer and weights-of-evidence models in landslide susceptibility mapping using GIS. *Geomat Nat Hazards Risk* 4(2):93–118. doi:10.1080/19475705.2012.662915
- Pourghasemi HR, Pradhan B, Gokceoglu C (2012c) Application of fuzzy logic and analytical hierarchy process (AHP) to landslide susceptibility mapping at Haraz watershed, Iran. *Nat Hazards* 63(2):956–996
- Pradhan B (2010a) Remote sensing and GIS-based landslide hazard analysis and cross validation using multivariate logistic regression model on three test areas in Malaysia. *Adv Space Res* 45:1244–1256
- Pradhan B (2010b) Application of an advanced fuzzy logic model for landslide susceptibility analysis. *Int J Comput Intell Syst* 3:370–381
- Pradhan B (2010c) A comparative study on the predictive ability of the decision tree, support vector machine and neuro-fuzzy models in landslide susceptibility mapping using GIS. *Comput Geosci* 51(2):350–365
- Pradhan B (2011a) Manifestation of an advanced fuzzy logic model coupled with geoinformation techniques for landslide susceptibility analysis. *Environ Ecol Stat* 18(3):471–493
- Pradhan B (2011b) Use of GIS-based fuzzy logic relations and its cross application to produce landslide susceptibility maps in three test areas in Malaysia. *Environ Earth Sci* 63(2):329–349
- Pradhan B, Lee S (2007) Utilization of optical remote sensing data and GIS tools for regional landslide hazard analysis using an artificial neural network model. *Earth Sci Front* 14(16):143–152
- Pradhan B, Lee S, Mansor S, Buchroithner MF, Jallaluddin N, Khujaimah Z (2008) Utilization of optical remote sensing data and geographic information system tools for regional landslide hazard analysis by using binomial logistic regression model. *J Appl Remote Sens* 2(1):142–154
- Pradhan B, Sezer EA, Gokceoglu C (2010) Landslide susceptibility mapping by neuro-fuzzy approach in a landslide-prone area (Cameron Highlands, Malaysia). *IEEE Trans Geosci Remote Sens* 48(12):4164–4177
- Rowbotham DN, Dudyca D (1998) GIS modelling of slope stability in Phewa Tal watershed. Nepal. *Geomorphology* 26(1):151–170
- Rupke J, Cammeraat E, Seijmonsbergen A, Van WC (1988) Engineering geomorphology of Widentobel Catchment, Appenzell and Sankt Gallen, Switzerland: a geomorphological inventory system applied to geotechnical appraisal of slope stability. *Eng Geol* 26:33–68
- Saaty TL (1977) A scaling method for priorities in hierarchical structures. *J Math Psychol* 15:234–281
- Saaty TL (1980) *The analytical hierarchy process*. McGraw-Hill, New York
- Saaty TL (2000) Decision making for leaders: the analytical hierarchy process for decisions in a complex world. *Eur J Oper Res* 129(4):275–286
- Saaty TL, Vargas GL (2001) *Models, methods, concepts, and applications of the analytic hierarchy process*. Kluwer Academic Publisher, London
- Saha AK, Gupta RP, Arora MK (2002) GIS-based landslide hazard zonation in the Bhagirathi (Ganga) valley, Himalayas. *Int J Remote Sens* 23(2):357–369
- Saha AK, Gupta RP, Sarkar I, Arora MK, Casplovics E (2005) An approach for GIS-based statistical landslide susceptibility zonation with a case study in the Himalayas. *Landslides* 2:61–69
- Santacana N, Baeza B, Corominas J, Paz A, Marturia J (2003) A GIS-based multivariate statistical analysis for shallow landslide susceptibility mapping in La Pobla de Lillet Area (Eastern Pyrenees, Spain). *Nat Hazards* 30(3):281–295
- Sassa Kyoji, Tsuchiya Satoshi, Ugai Keizo, Wakai Akihiko, Uchimur Tarō (2009) Landslides: a review of achievements in the first 5 years (2004–2009). *Landslides* 6(4):275–286
- Scholkopf B, Smola A, Williamson RC, Bartlett PL (2000) New Support vector algorithms. *Neural Comput* 12:1207–1245
- Schumacher M, Robner R, Vach W (1996) neural networks and logistic regression. Part I. *Comput Stat Data Anal* 21:661–682
- Sezer EA, Pradhan B, Gokceoglu C (2011) Manifestation of an adaptive neuro-fuzzy model on landslide susceptibility mapping: Klang valley, Malaysia. *Expert Syst Appl* 38(7):8208–8219
- Sujatha ER, Kumaravel P, Victor RG (2012) Landslide susceptibility mapping using remotely sensed data through conditional probability analysis using seed cell and point sampling techniques. *J Indian Soc Remote Sens* 40(4):669–678
- Süzen ML, Doyuran V (2004) A comparison of the GIS based landslide susceptibility assessment methods: multivariate versus bivariate. *Environ Geol* 45(5):665–679
- Süzen ML, Kaya BS (2012) Evaluation of environmental parameters in logistic regression models for landslide susceptibility mapping. *Int J Digit Earth* 5(4):338–355
- Swets JA (1988) Measuring the accuracy of diagnostic systems. *Science* 240:1285–1293
- Talebi A, Uijlenhoet R, Troch PA (2007) Soil moisture storage and hill slopes stability. *Nat Hazards Earth Syst Sci* 7(5):523–534
- Tehrany MS, Pradhan B, Iebur MN (2013) Spatial prediction of flood susceptible areas using rule based decision tree and ensemble bivariate and multivariate statistical models. *J Hydrol* 504:69–79
- Tien BD, Pradhan B, Lofman O (2012) Landslide susceptibility mapping at Hoa Binh province (Vietnam) using an adaptive neuro-fuzzy inference system and GIS. *Comput Geosci* 45(4):199–211
- Tu JV (1996) Advantages and disadvantages of using artificial neural networks versus logistic regression for predicting medical outcomes. *Clin Epidemiol* 49(11):1225–1231
- UNESCO World Heritage Center (2006) Sichuan giant panda sanctuaries- Wolong, Mt Siguniang and Jiayin Mountains. <http://whc.unesco.org/en/list/1213>. Accessed 23 June 2006
- Vahidnia MH, Alesheikh AA, Alimohammadi A, Hosseinali F (2010) A GIS-based neuro-fuzzy procedure for integrating knowledge and data in landslide susceptibility mapping. *Comput Geosci* 36:1101–1114
- Vapnik V (1995) *The nature of statistical learning theory*. John Wiley and Sons, New York
- Varnes DJ (1978) *Slope movement types and processes*. Transportation Research Board Special Report, New York
- Wilson JP, Gallant JC (2000) *Terrain analysis: principles and applications*. Wiley, New York

- Xu C, Xu XW, Yao Q, Wang YY (2013) GIS-based bivariate statistical modelling for earthquake-triggered landslides susceptibility mapping related to 2008 Wenchuan earthquake, China. *Q J Eng Geol Hydrogeol* 46(2):221–236. doi:10.1144/qjegh2012-006
- Yalcin A, Reis S, Aydinoglu AC (2011) A GIS-based comparative study of frequency ratio, analytical hierarchy process, bivariate statistics and logistics regression methods for landslide susceptibility mapping in Trabzon, NE Turkey. *Catena* 85(3):274–287
- Yao X, Tham LG, Dai FC (2008) Landslide susceptibility mapping based on support vector machine: a case study on natural slopes of Hong Kong, China. *Geomorphology* 101(4):572–582
- Yesilnacar E, Topal T (2005) Landslide susceptibility mapping: a comparison of logistic regression and neural networks methods in a medium scale study, Hendek region (Turkey). *Eng Geol* 79(3–4):251–266
- Yilmaz I (2008) A case study from Koyulhisar (Sivas-Turkey) for landslide susceptibility mapping by artificial neural networks. *Bull Eng Geol Environ* 68(3):297–306
- Yilmaz I (2009) Landslide susceptibility mapping using frequency ratio, logistic regression, artificial neural networks and their comparison: a case study from Kat landslides (Tokat-Turkey). *Comput Geosci* 35(6):1125–1138
- Yilmaz I (2010a) Comparison of landslide susceptibility mapping methodologies for Koyulhisar, Turkey: conditional probability, logistic regression, artificial neural networks, and support vector machine. *Environ Earth Sci* 61(4):821–836
- Yilmaz I (2010b) The effect of the sampling strategies on the landslide susceptibility mapping by conditional probability (CP) and artificial neural networks (ANN). *Environ Earth Sci* 60(3):505–519
- Yilmaz I, Yildirim M (2006) Structural and geomorphological aspects of the Kat landslides (Tokat-Turkey) and susceptibility mapping by means of GIS. *Environ Geol* 50(4):461–472
- Yilmaz I, Yuksek AG (2008a) An example of artificial neural network (ANN) application for indirect estimation of rock parameters. *Rock Mech Rock Eng* 41(5):781–795
- Yilmaz I, Yuksek AG (2008b) Prediction of the strength and elasticity modulus of gypsum using multiple regression, ANN, and ANFIS models. *Int J Rock Mech Min Sci* 46(4):803–810
- Yilmaz C, Topal T, Süzen ML (2012) GIS-based landslide susceptibility mapping using bivariate statistical analysis in Devrek (Zonguldak-Turkey). *Environ Earth Sci* 65(7):2161–2178
- Yoshimatsu H, Abe S (2006) A review of landslide hazards in Japan and assessment of their susceptibility using an analytical hierarchic process (AHP) method. *Landslides* 3(2):149–158
- Zadeh LA (1965) Fuzzy sets. *Inf Control* 8:338–352